SENSORCOMM 2023

The Seventeenth International Conference on Sensor Technologies and Applications

ISBN: 978-1-68558-090-2

September 25 - 29, 2023

Porto, Portugal

SENSORCOMM 2023 Editors

Sandra Sendra Compte, Universitat Politècnica de València, Spain

SENSORCOMM 2023

Forward

The Seventeenth International Conference on Sensor Technologies and Applications (SENSORCOMM 2023), held on September 25-29, 2023, was a multi-track event covering related topics on theory and practice on wired and wireless sensors and sensor networks.

Sensors and sensor networks have become a highly active research area because of their potential of providing diverse services to broad range of applications, not only on science and engineering, but equally importantly on issues related to critical infrastructure protection and security, health care, the environment, energy, food safety, and the potential impact on the quality of all areas of life.

Sensor networks and sensor-based systems support many applications today on the ground. Underwater operations and applications are quite limited by comparison. Most applications refer to remotely controlled submersibles and wide-area data collection systems at a coarse granularity.

In wireless sensor and micro-sensor networks energy consumption is a key factor for the sensor lifetime and accuracy of information. Protocols and mechanisms have been proposed for energy optimization considering various communication factors and types of applications. Conserving energy and optimizing energy consumption are challenges in wireless sensor networks, requiring energy-adaptive protocols, self-organization, and balanced forwarding mechanisms.

We take here the opportunity to warmly thank all the members of the SENSORCOMM 2023 technical program committee, as well as all the reviewers. The creation of such a high quality conference program would not have been possible without their involvement. We also kindly thank all the authors who dedicated much of their time and effort to contribute to SENSORCOMM 2023. We truly believe that, thanks to all these efforts, the final conference program consisted of top quality contributions.

We also thank the members of the SENSORCOMM 2023 organizing committee for their help in handling the logistics and for their work that made this professional meeting a success.

We hope that SENSORCOMM 2023 was a successful international forum for the exchange of ideas and results between academia and industry and to promote further progress in the area of sensor technologies and applications. We also hope that Porto provided a pleasant environment during the conference and everyone saved some time to enjoy the historic charm of the city.

SENSORCOMM 2023 Chairs

SENSORCOMM 2023 Steering Committee
Anne-Lena Kampen, Western Norway University of Applied Sciences, Norge
Masanari Nakamura, Hokkaido University, Japan

SENSORCOMM 2023 Publicity Chair
Lorena Parra Boronat, Universitat Politecnica de Valencia, Spain
Laura Garcia, Universitat Politecnica de Valencia, Spain

SENSORCOMM 2023

Committee

SENSORCOMM 2023 Steering Committee
Anne-Lena Kampen, Western Norway University of Applied Sciences, Norge
Masanari Nakamura, Hokkaido University, Japan

SENSORCOMM 2023 Publicity Chair
Lorena Parra Boronat, Universitat Politecnica de Valencia, Spain
Laura Garcia, Universitat Politecnica de Valencia, Spain

SENSORCOMM 2023 Technical Program Committee

Majid Bayani Abbasy, National University of Costa Rica, Costa Rica
Younes Adriouch, Mohammed Five University of Rabat (UM5R), Agdal, Rabat, Morocco
Yassine Al-Amrani, Abdelmalek Essaadi University, Tetuan, Morocco
Amin Al-Habaibeh, Nottingham Trent University, UK
Jesús B. Alonso Hernández, Institute for Technological Development and Innovation in Communications (IDeTIC) | University of Las Palmas de Gran Canaria (ULPGC), Spain
Youssef N. Altherwy, Imperial College London, UK
Mário Alves, Politécnico do Porto - School of Engineering (ISEP), Portugal
Thierry Antoine-Santoni, University of Corsica, France
Kazutami Arimoto, Okayama Prefectural University, Japan
Anish Arora, The Ohio State University / The Samraksh Company, USA
Andy Augousti, Kingston University London, UK
Karim Baïna, Université Mohammed V de Rabat, Morocco
Michel Bakni, ESTIA Recherche, Bidart, France
Hind Bangui, Masaryk University, Czech Republic
Michail J. Beliatis, Aarhus University, Denmark
Boutaina Benhmimou, Mohammed Five University of Rabat (UM5R), Agdal, Rabat, Morocco
Reda Benkhouya, Ibn Tofail University, Morocco
Abdelmadjid Bouabdallah, University of Technology of Compiegne, France
Souheila Bouam, University of Batna 2, Algeria
An Braeken, Vrije Universiteit België, Belgium
Seddik Bri, Higher School of Technology - Moulay Ismail University, Meknes, Morocco
Juan-Vicente Capella-Hernández, Universitat Politècnica de València, Spain
Oscar Carrasco Quilis, Casa Systems Inc., Valencia, Spain
Vítor Carvalho, 2Ai Lab- School of Technology - IPCA / Algoritmi Research Center - Minho University, Portugal
Mario Cifrek, University of Zagreb, Croatia
Luis J. de la Cruz Llopis, Universitat Politècnica de Catalunya, Spain
Baban P. Dhonge, Indira Gandhi Center for Atomic Research, Kalpakkam, India
Alexis Duque, Rtone, Lyon, France
Nabil El Akkad, ENSA | Sidi Mohamed Ben Abdellah University, Morocco
Loubna El Amrani, Ibn University Tofail Kénitra, Morocco

Sergey Y. Yurish, International Frequency Sensor Association (IFSA), Spain
Zhenghao Zhang, Florida State University, USA
Zhe Zhou, Huzhou University, China
Chengzhi Zong, eBay Inc, USA

Table of Contents

Cooperative Tracking of People Using Networked LiDARs

Marino Matsuba, Ryota Imai
Graduate School of Science and Engineering
Doshisha University
Kyotanabe, Kyoto, 610-0394 Japan
e-mail: {ctwh0137, ctwj0109}@mail4.doshisha.ac.jp

Masafumi Hashimoto, Kazuhiko Takahashi
Faculty of Science and Engineering
Doshisha University
Kyotanabe, Kyoto, 610-0394 Japan
e-mail: {mhashimo, katakaha}@mail. doshisha.ac.jp

***Abstract*—This paper presents a tracking method of people using networked Light Detection And Ranging sensors (LiDARs) set in an environment. Each LiDAR detects people from the LiDAR scan data using a background subtraction method and sends the positions of the people to the neigboring LiDARs. It estimates the people's positions and velocities and exchanges information with the neigboring LiDARs. A Distributed Interacting MultiModel (DIMM)-based method is used to accurately estimate people's positions and velocities under various motion modes, such as stopping, walking, and suddenly running, in a distributed manner without a central server. Simulation experiments of the tracking of 20 people using three Velodyne 32-layer LiDARs are conducted in two different network topologies (ring and line network topologies) to quantitatively evaluate the tracking performance and computation effort of the proposed method. Simulation results show that the tracking performance and computation time of the DIMM-based method are comparable to those of conventional centralized interacting multimodel-based method.**

Keywords—LiDAR; people tracking; cooperative tracking; diffusion strategy; interacting multimodel estimator.

I. INTRODUCTION

Estimating the motion and behavior (*i.e.*, tracking) of moving objects, such as people, cars, and two-wheelers, in an environment is vital in several applications, including Intelligent Transport Systems (ITS), autonomous driving, security, and surveillance. Therefore, many tracking systems based on Light Detection And Ranging sensors (LiDARs) and cameras have been developed [1]–[3]. In this paper, we investigate people tracking using LiDARs allocated in an environment.

In sparsely populated environments, LiDAR-based tracking of people is efficient. However, its performance in crowded environments is poor because of occlusions. An effective method for accurately tracking people in crowded environments is the use of networked multiple LiDARs. Despite occasions where people are occluded or are located outside a surveillance area of a LiDAR, the use of networked multiple LiDARs (referred to as cooperative tracking) improves tracking reliability and accuracy as tracking data are shared among LiDARs [4][5].

For the application of cooperative tracking to ITS domains, we proposed cooperative tracking of people using networked multiple ground LiDARs allocated to different locations in an intersection environment [6]. The cooperative tracking method detects people's positions, velocities, and behavior, such as stopping, walking, and suddenly running. Usual algorithms for people tracking are based on Bayesian filters and assume that people walk or run at an almost constant speed. Therefore, when people suddenly change their motions, such as suddenly running, turning, or stopping, the tracking accuracy decreases. To accurately track people under such conditions, we proposed a multimodel-based approach, which employs an Interacting MultiModel (IMM) estimator [7], instead of the single-model Kalman filter approach.

Most studies on cooperative tracking employ centralized data fusion with a central server, in which sensing data are captured and preprocessed by each sensor, sent to a central server, and then fused in the central server [4][5]. In the first version of our cooperative tracking system [6][8], a Centralized Interacting MultiModel (CIMM) estimator [9] was employed to estimate people's positions, velocities, and behavior by the central server.

Centralized data fusion reduces system robustness and scalability. Recently, various methods for distributed state estimation have been proposed in the field of Bayesian filtering [10][11], in which information processing among multiple sensors is distributed among sensors without using a central server. Thus, in our previous study [12], we proposed cooperative tracking of people that functions in a distributed manner without any central servers, and a Distributed Interacting MultiModel (DIMM) estimator [13] was employed. However, people could be tracked using only two LiDARs.

In this paper, DIMM-based cooperative tracking of people is presented using three LiDARs. The contributions of this paper are as follows:

- A DIMM-based cooperative people tracking method using three LiDARs are designed in two different network topologies (ring and line network topologies). The tracking method is applicable to four or more LiDARs systems in any network topology.
- The tracking performance and computational effort of the presented DIMM-based method are quantitatively evaluated by comparing conventional CIMM-based and Kalman filter-based methods.

The rest of this paper is organized as follows: Section II gives an overview of the experimental system. Section III models people's motion, and Sections IV and V describe the people detection and tracking methods, respectively. Section VI presents the simulation conducted to evaluate the performance of the proposed cooperative tracking system. Section VII concludes the paper.

II. EXPERIMENTAL SYSTEM

Figure 1 shows our experimental system, which consists of three LiDARs. Each LiDAR has a 32-layer LiDAR (Velodyne HDL-32E) and a computer. The maximum range of the LiDAR is 50 m. The horizontal and vertical viewing angles are 360° and 41.3° with resolutions of 0.16° and 1.33°, respectively. The scanning period is 0.1 s.

Two network topologies can be considered for exchanging information among LiDARs: a ring network topology (referred to as a ring network) and a line network topology (a line network). As shown in Figure 1, each LiDAR is connected to two other adjacent LiDARs in the ring network, whereas, in the line network, LiDARs 1 and 2 and LiDARs 2 and 3 are connected.

For four or more LiDARs, similar to the case of three LiDARs, each LiDAR is connected to two other LiDARs on both sides in a ring network, whereas, in a line network, only the LiDARs at both ends of the line are connected to one adjacent LiDAR, and other LiDARs are connected to the two LiDARs.

III. MOTION AND MEASUREMENT MODELS OF A PERSON

To accurately track people in an intersection environment, we consider three motion modes of a person as follows [8]:

- Stop mode (mode 1): A person stops.
- Constant velocity mode (mode 2): A person walks or runs at an almost constant velocity.
- Sudden motion mode (mode 3): A person starts to suddenly run or stops suddenly.

A person's position is denoted by (x, y), and the moving direction of the person is denoted by θ. The translational and turning velocities of the person are denoted by v and $\dot{\theta}$, respectively. The three motion modes are then modeled by the following state equations:

- Mode 1

$$\begin{bmatrix} x_t \\ y_t \end{bmatrix} = \begin{bmatrix} x_{t-1} + \Delta\dot{x}_{t-1}\tau \\ y_{t-1} + \Delta\dot{y}_{t-1}\tau \end{bmatrix} \tag{1}$$

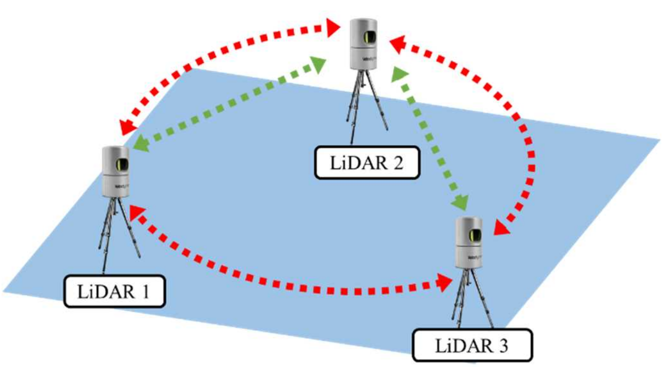

Figure 1. Overview of the networked three LiDARs. The red and green dotted lines indicate ring and line network topologies, respectively.

- Mode 2

$$\begin{bmatrix} x_t \\ y_t \\ \theta_t \\ v_t \\ \dot{\theta}_t \end{bmatrix} = \begin{bmatrix} x_{t-1} + (v_{t-1}\tau + \frac{1}{2}\Delta\dot{v}_{t-1}\tau^2)\cos\theta_{t-1} \\ y_{t-1} + (v_{t-1}\tau + \frac{1}{2}\Delta\dot{v}_{t-1}\tau^2)\sin\theta_{t-1} \\ \theta_{t-1} + \dot{\theta}_{t-1}\tau + \frac{1}{2}\Delta\ddot{\theta}_{t-1}\tau^2 \\ v_{t-1} + \Delta\dot{v}_{t-1}\tau \\ \dot{\theta}_{t-1} + \Delta\ddot{\theta}_{t-1}\tau \end{bmatrix} \tag{2}$$

- Mode 3

$$\begin{bmatrix} x_t \\ y_t \\ \theta_t \\ v_t \\ \dot{v}_t \end{bmatrix} = \begin{bmatrix} x_{t-1} + (v_{t-1}\tau + \frac{1}{2}\dot{v}_{t-1}\tau^2 + \frac{1}{6}\Delta\ddot{v}_{t-1}\tau^3)\cos\theta_{t-1} \\ y_{t-1} + (v_{t-1}\tau + \frac{1}{2}\dot{v}_{t-1}\tau^2 + \frac{1}{6}\Delta\ddot{v}_{t-1}\tau^3)\sin\theta_{t-1} \\ \theta_{t-1} + \Delta\dot{\theta}_{t-1}\tau \\ v_{t-1} + \dot{v}_{t-1}\tau + \frac{1}{2}\Delta\ddot{v}_{t-1}\tau^2 \\ v_{t-1} + \Delta\ddot{v}_{t-1}\tau \end{bmatrix} \tag{3}$$

where t and t-1 indicate time steps. $\dot{v}$ and $\ddot{\theta}$ are the translational and turning accelerations of the person, respectively. $\Delta\dot{x}$, $\Delta\dot{y}$, $\Delta\dot{v}$, $\Delta\ddot{v}$, $\Delta\dot{\theta}$ and $\Delta\ddot{\theta}$ are the plant disturbances. τ (= 100 ms) is the sampling period of the LiDAR.

For simplicity, the state equation of the m-th mode (m = 1, 2, 3) is represented by the following vector form:

$$\boldsymbol{x}_t^m = \boldsymbol{f}^m(\boldsymbol{x}_{t-1}^m, \Delta\boldsymbol{v}_{t-1}^m) \tag{4}$$

where $\boldsymbol{x}^m$ is the state vector, and $\Delta\boldsymbol{v}^m$ is the plant disturbance vector, which is assumed to have a white noise sequence with the covariance matrix $\boldsymbol{Q}^m$.

The LiDAR measurement related to a person gives the following equation:

$$\boldsymbol{z}_t = \boldsymbol{H}^m\boldsymbol{x}_t^m + \Delta\boldsymbol{z}_t \tag{5}$$

where $\boldsymbol{z} = (z_x, z_y)^T$ is the position of the person. $\Delta\boldsymbol{z}$ is the measurement noise, which is assumed to have a white noise sequence with the covariance matrix $\boldsymbol{R}$. $\boldsymbol{H}^m$ is the measurement matrix.

IV. PEOPLE DETECTION USING BACKGROUND SUBTRACTION METHOD

Figure 2 shows the sequence of people detection and tracking. Each LiDAR captures its own scan data and maps them onto an elevation map. In the elevation map, a cell containing two or more scan data is called an occupied cell. Each LiDAR extracts the occupied cell related to a person (referred to as a person-cell) based on the background subtraction method. Generally, the LiDAR scan data related to a person occupy two or more cells, and the neighboring person cells are clustered (referred to as person-cell group).

Each LiDAR communicates with the adjacent LiDAR and exchanges the information of clustered person cells. Thereafter, each LiDAR fuses the information of person cells and then determines the geometric center of person cells as the

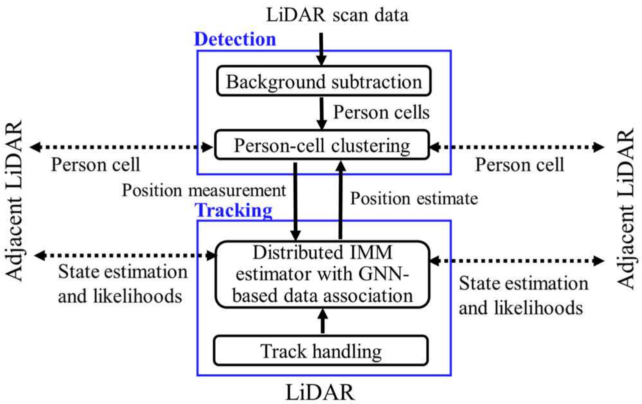

Figure 2. Sequence of people detection and tracking.

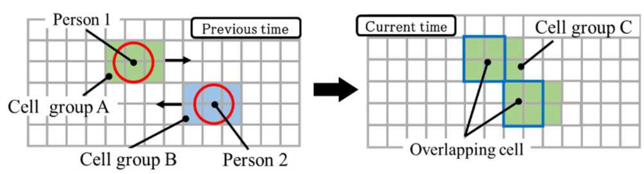

(a) Cell merging

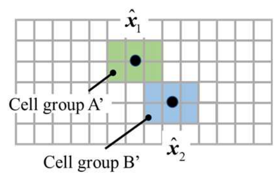

(b) Cell splitting

Figure 3. Cell merging and splitting of two passing people (top view).

person's position.

In our simulation, the cell size of the elevation map is set to 0.3 m. Therefore, when the distance of neighboring two people is less than 0.3 m, two person-cell groups are merged, and the people are detected as a person. To address this problem, the merged person-cell groups are split, as described below.

Consider two people passing each other. Figure 3 shows the person cells for such people on the elevation map. Initially, two person-cell groups A and B for persons 1 and 2, respectively, are extracted, and at the current time, the person-cell groups are merged into C. We examine whether the cells in person-cell groups A and B partially overlap those in person-cell group C. If the cells overlap, as those in a blue frame in Figure 3(a), the two person-cell groups are considered to have merged. Then, the merged person-cell group C is split to accurately track the two people.

The coordinates of each cell in the merged person-cell group C are compared with the positions $\hat{\boldsymbol{x}}_1$ and $\hat{\boldsymbol{x}}_2$ of persons 1 and 2, respectively, estimated at the initial time using our tracker. When the coordinate of the cell is near $\hat{\boldsymbol{x}}_1$ ($\hat{\boldsymbol{x}}_2$), the cell is classified as a person-cell group A' (B') related to person 1 (2). Thereafter, the geometrical centers of the person-cell groups A' and B' are obtained as the positions of persons 1 and 2, respectively.

V. DIMM-BASED COOPERATIVE TRACKING

A sequence of the above-mentioned motion modes is assumed to be governed by the first-ordered homogeneous Markov chain as follows:

$$T_{mn} = \text{Prob}\left\{\pi_t^n \,\middle|\, \pi_{t-1}^m\right\} \tag{6}$$

$$\sum_{n=1}^{3} T_{mn} = 1 \tag{7}$$

where π_{t-1}^m and π_t^n are events that the m-th and n-th modes (m, n = 1, 2, 3) are in effect at times t–1 and t, respectively. T_{mn} is the transition probability that the m-th mode jumps into the n-th mode. In our simulation, the transition probability matrix is set to T_{mn} = 0.9 for $m = n$ and 0.05 for $m \neq n$.

The k-th LiDAR (k = 1, 2, 3) estimates people's state in the following five steps [12][13]:

Step 1) Filter initialization: The probability that the m-th mode occurs at time t–1 is denoted by $\hat{\mu}_{k,t-1}^m$. The m-th mode conditional estimate and its related covariance are denoted by $\hat{\boldsymbol{x}}_{k,t-1}^m$ and $\boldsymbol{P}_{k,t-1}^m$, respectively. The three quantities interact with one another as follows:

$$\hat{\mu}_{k,t/t-1}^n = \sum_{m=1}^{3} \boldsymbol{T}_{mn} \hat{\mu}_{k,t-1}^m \tag{8}$$

$$\bar{\boldsymbol{x}}_{k,t-1}^m = \sum_{n=1}^{3} c_{mn} \hat{\boldsymbol{x}}_{k,t-1}^n \tag{9}$$

$$\bar{\boldsymbol{P}}_{k,t-1}^m = \sum_{n=1}^{3} c_{k,mn} [\boldsymbol{P}_{t-1}^n + (\bar{\boldsymbol{x}}_{k,t-1}^m - \hat{\boldsymbol{x}}_{k,t-1}^n)(\bar{\boldsymbol{x}}_{k,t-1}^m - \hat{\boldsymbol{x}}_{k,t-1}^n)^T] \tag{10}$$

where $c_{k,mn} = T_{mn} \hat{\mu}_{k,t-1}^m / \hat{\mu}_{k,t/t-1}^n$

Step 2) State estimation: A bank of the single-model-based Kalman filters runs, and the prediction and its related covariance for each mode are updated:

$$\left.\begin{aligned} \hat{\boldsymbol{x}}_{k,t/t-1}^m &= \boldsymbol{f}^m(\bar{\boldsymbol{x}}_{k,t-1}^m) \\ \boldsymbol{P}_{k,t/t-1}^m &= \nabla \boldsymbol{F}_{t-1} \bar{\boldsymbol{P}}_{k,t-1}^m \nabla \boldsymbol{F}_{t-1}^T + \nabla \boldsymbol{G}_{t-1} \boldsymbol{Q}^m \nabla \boldsymbol{G}_{t-1}^T \end{aligned}\right\} \tag{11}$$

where $\nabla \boldsymbol{F}$ and $\nabla \boldsymbol{G}$ are Jacobian matrices of $\boldsymbol{f}^m$ ((4)) related to $\bar{\boldsymbol{x}}_{k,t-1}^m$ and $\Delta \boldsymbol{v}_{t-1}^m$, respectively.

By blending the measured position of people, $\boldsymbol{z}_k$, the quantities related to the measurement $\boldsymbol{q}_{k,t}$ and its error covariance $\boldsymbol{S}_{k,t}$ are given by

$$\left.\begin{aligned} \boldsymbol{q}_{k,t}^m &= \sum_{l \in N_k} (\boldsymbol{H}_l^m)^T \boldsymbol{R}_l^{-1} \boldsymbol{z}_{l,t} \\ \boldsymbol{S}_{k,t}^m &= \sum_{l \in N_k} (\boldsymbol{H}_l^m)^T \boldsymbol{R}_l^{-1} \boldsymbol{H}_l^m \end{aligned}\right\} \tag{12}$$

The state estimate $\boldsymbol{\gamma}_{k,t}^m$ and its related error covariance $\boldsymbol{\Gamma}_{k,t}^m$ at time t are determined using the information filter as follows:

$$\left.\begin{aligned} \boldsymbol{\gamma}_{k,t}^m &= (\boldsymbol{\Gamma}_{k,t}^m)^{-1} \{(\boldsymbol{P}_{k,t/t-1}^m)^{-1} \hat{\boldsymbol{x}}_{k,t/t-1}^m + \boldsymbol{q}_{k,t}^m\} \\ \boldsymbol{\Gamma}_{k,t}^m &= \{(\boldsymbol{P}_{k,t/t-1}^m)^{-1} + \boldsymbol{S}_{k,t}^m\}^{-1} \end{aligned}\right\} \tag{13}$$

In (12), N_k is the set of neighboring LiDARs, including itself (i.e., k-th LiDAR). In the ring network, N_1=N_2=N_3={1, 2, 3}, and in the line network, N_1={1, 2}, N_2={1, 2, 3}, and N_3={2, 3}.

 ISBN: 978-1-68558-090-2

The model-conditional likelihood is calculated by

$$\phi_{k,t}^{m}=\prod_{l\in N_k}\frac{1}{\sqrt{2\pi}\left|\boldsymbol{L}_{k,t/t-1}^{m}\right|}\exp[-\frac{1}{2}(\tilde{\boldsymbol{z}}_{k,t/t-1}^{m})^{T}(\boldsymbol{L}_{k,t/t-1}^{m})^{-1}\tilde{\boldsymbol{z}}_{k,t/t-1}^{m}] \tag{14}$$

where the predicted measurement error $\tilde{\boldsymbol{z}}_{k,t/t-1}^{m}$ and its associated covariance $\boldsymbol{L}_{k,t/t-1}^{m}$ are given by

$$\left.\begin{aligned}\tilde{\boldsymbol{z}}_{k,t/t-1}^{m}&=\boldsymbol{z}_{k,t}-\boldsymbol{H}_{k}^{m}\hat{\boldsymbol{x}}_{k,t/t-1}^{m}\\ \boldsymbol{L}_{k,t/t-1}^{m}&=\boldsymbol{H}_{k}^{m}\boldsymbol{P}_{k,t/t-1}^{m}(\boldsymbol{H}_{k}^{m})^{T}+\boldsymbol{R}\end{aligned}\right\} \tag{15}$$

Step 3) Exchange of tracking information and likelihood: All LiDARs communicate with one another and exchange information about the state estimate $\boldsymbol{\gamma}_{k,t}^{m}$, its related error covariance $\boldsymbol{\Gamma}_{k,t}^{m}$, and the model-conditional likelihood $\phi_{k,t}^{m}$.

Step 4) Integration of tracking information: By integrating the tracking information exchanged among LiDARs in Step 3, the *m*-th model-conditional estimate $\hat{\boldsymbol{x}}_{k,t}^{m}$ and its related covariance $\boldsymbol{P}_{k,t}^{m}$ at time *t* are given by

$$\left.\begin{aligned}\hat{\boldsymbol{x}}_{k,t}^{m}&=\boldsymbol{P}_{k,t}^{m}\{\sum_{l\in N_k}\alpha_{lk,t}^{m}(\boldsymbol{\Gamma}_{k,t}^{m})^{-1}\boldsymbol{\gamma}_{k,t}^{m}\}\\ (\boldsymbol{P}_{k,t}^{m})^{-1}&=\sum_{l\in N_k}\alpha_{lk,t}^{m}(\boldsymbol{\Gamma}_{k,t}^{m})^{-1}\end{aligned}\right\} \tag{16}$$

where the weight $\alpha_{lk,t}^{m}$ is set so that the smaller the state estimation error covariance $\boldsymbol{\Gamma}_{l,t}^{m}$ is, the larger the weight:

$$\alpha_{lk,t}^{m}=\begin{cases}\dfrac{\dfrac{1}{\mathrm{Tr}(\boldsymbol{\Gamma}_{k,t}^{m})}}{\sum_{l\in N_k}\dfrac{1}{\mathrm{Tr}(\boldsymbol{\Gamma}_{l,t}^{m})}} & \text{for } l\in N_k\\ 0 & \text{for } l\notin N_k\end{cases} \tag{17}$$

Step 5) Update of mode probability: Based on the likelihood $\phi_{k,t}^{m}$ exchanged among LiDARs in step 3, the likelihood function of the *m*-th mode, $\Lambda_{k,t}^{m}$, is integrated by

$$\log\Lambda_{k,t}^{m}=\sum_{l\in N_k}\beta_{lk}^{m}\log\phi_{k,t}^{m} \tag{18}$$

The weight β_{lk}^{m} is given by [14]

$$\beta_{lk}^{m}=\begin{cases}\dfrac{1}{\max\left(\left|N_l\right|,\left|N_k\right|\right)} & \text{for } l\in N_k, l\neq k\\ 1-\sum_{l\in N_k, l\neq k}\beta_{lk}^{m} & \text{for } l=k\\ 0 & \text{for } l\notin N_k\end{cases} \tag{19}$$

where $\left|N_l\right|$ and $\left|N_k\right|$ are the dimensions of N_l and N_k, respectively.

The mode probability is therefore calculated as follows:

$$\hat{\mu}_{k,t}^{m}=\frac{\hat{\mu}_{k,t/t-1}^{m}\Lambda_{t}^{m}}{\sum_{m=1}^{3}\hat{\mu}_{k,t/t-1}^{m}\Lambda_{k,t}^{m}} \tag{20}$$

Using the mode probability, we recognize the motion mode that occurs.

Step 6) Calculation of state estimates: The state estimate and its related error covariances of tracked people are given by

$$\left.\begin{aligned}\hat{\boldsymbol{x}}_{k,t}&=\sum_{m=1}^{3}\hat{\mu}_{k,t}^{m}\hat{\boldsymbol{x}}_{k,t}^{m}\\ \boldsymbol{P}_{k,t}&=\sum_{m=1}^{3}\hat{\mu}_{k,t}^{m}[\boldsymbol{P}_{k,t}^{m}+(\hat{\boldsymbol{x}}_{k,t}-\hat{\boldsymbol{x}}_{k,t}^{m})(\hat{\boldsymbol{x}}_{k,t}-\hat{\boldsymbol{x}}_{k,t}^{m})^{T}]\end{aligned}\right\} \tag{21}$$

In steps 2 and 4, to accurately track many people, each LiDAR sets a validation region around the predicted position of each tracked person [15]. LiDAR measurements (measurements of person's position) within the validation region, which are obtained from the tracked person, are applied to the track update. In crowded environments, multiple LiDAR measurements are within a validation region, and several validation regions overlap. To achieve reliable data association (matching of tracked people and LiDAR measurements), the global-nearest-neighbor-based data association [16] is exploited. The number of people in the sensing areas of LiDARs changes over time. They often encounter occlusions. To handle such conditions, a rule-based data-handling method, which employs track initiation and termination [15], is implemented.

VI. SIMULATION EXPERIMENTS

As shown in Figure 4 (a), three LiDARs are placed in an intersection environment, and 20 people are tracked. People's motions and LiDAR scan data are generated by a simulator (Siemens, Simcenter Prescan). Figure 4 (b) shows the paths taken by 20 people. People that moved along the blue paths walked at 1.5 m/s and then stopped. People that moved along the red paths walked at 1.2 m/s and then stopped. People that moved along the purple paths walked at 1.5 m/s from a stop, ran at 3.0 m/s, and then stopped. As an example, Figure 5 shows the velocity profiles of seven of the 20 people.

The tracking performance is evaluated for the following four cases.

- Case 1: DIMM-based tracking in a ring network,
- Case 2: DIMM-based tracking in a line network,
- Case 3: CIMM-based tracking,
- Case 4: Distributed Kalman filter (DKF)-based tracking in a ring network.

In case 3, the person cells detected by the three LiDARs are collected on a central server, and the central server tracks people using a conventional IMM estimator [6][8]. In case 4, only the constant speed model ((2)) is used as a motion model of a person.

Figure 6 shows the tracking results for person 1 in cases 1 and 2, and Figure 7 shows those in cases 1 and 3. Table I lists the tracking errors for the 20 people. In the table, the result for case 1 shows the following root-mean-squared error J_i for the *i*-th person (i = 1 to 20):

$$J_i=\sqrt{\frac{1}{N}\sum_{t=0}^{N}(\Delta\hat{x}_{it}^{2}+\Delta\hat{y}_{it}^{2}+\Delta\hat{v}_{it}^{2}+\Delta\hat{\theta}_{it}^{2})} \tag{22}$$

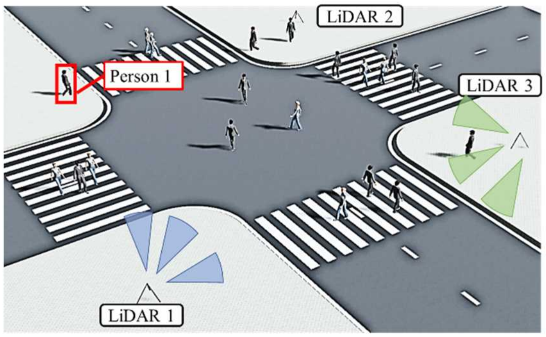

(a) Bird's-eye view

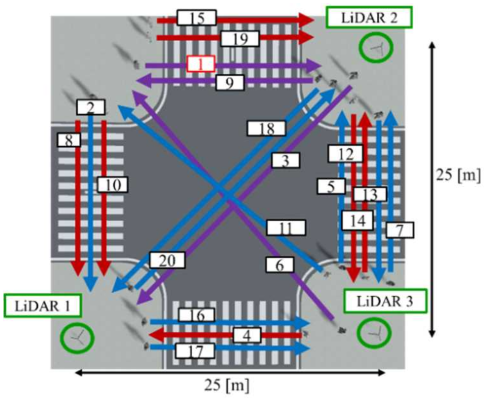

(b) Top view

Figure 4. Simulation environment and paths taken by 20 people.

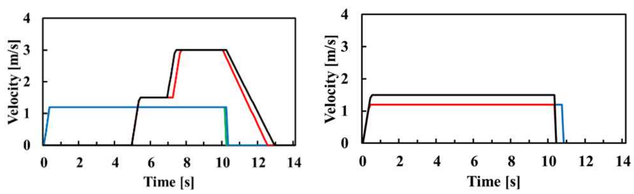

(a) Persons 1(black), 9 (red), 15 (blue) and 19 (green).

(b) Persons 2 (black), 8 (red), and 10 (blue).

Figure 5. Velocity profile of people. The blue and green lines in (a) significantly overlap, and the red and blue lines in (b) significantly overlap.

where ($\Delta\hat{x}_{it}$, $\Delta\hat{y}_{it}$), $\Delta\hat{v}_{it}$, and $\Delta\hat{\dot{\theta}}_{it}$ are estimate errors in a position, translational velocity, and turn velocity, respectively. N is the tracking duration.

On the other hand, the results for cases 2, 3, and 4 represent the percentage of the tracking error to that in case 1. Thus, the positive sign (+) indicates that the tracking error is larger than that for case 1, whereas the negative sign (-) indicates the opposite.

As listed in Table I, the tracking error in case 2 (line network) is approximately 8 % larger than that in case 1 (ring network). This is because in case 1, each LiDAR exchanges detection and tracking information with two LiDARs located at both sides, whereas, in case 2, LiDARs 1 and 3 exchange information only with LiDAR 2. Since the difference in the tracking error between case 1 (DIMM-based tracking) and case 3 (CMM-based tracking) is approximately 1 %, both methods can track people at almost the same degree of accuracy.

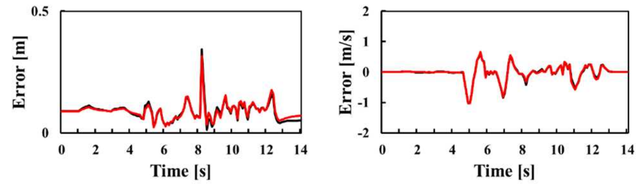

(a) Position (b) Translation velocity

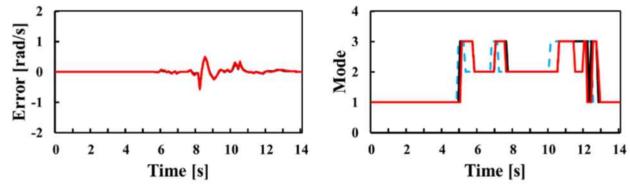

(c) Turn velocity (d) Mode estimate

Figure 6. Tracking error in cases 1 (black) and 2 (red). The blue dashed line in (d) indicates the true mode.

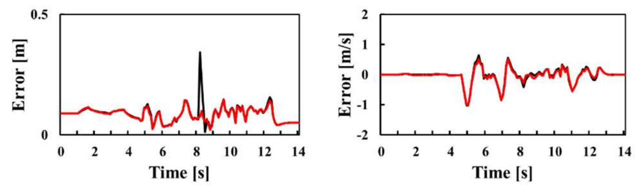

(a) Position (b) Translation velocity

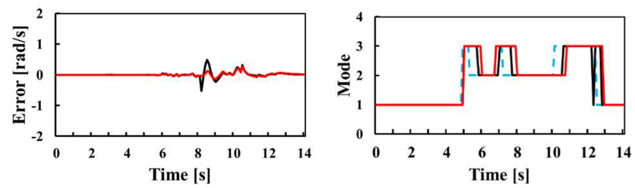

(c) Turn velocity (d) Mode estimate

Figure 7. Tracking error in cases 1 (black) and 3 (red). The blue dashed line in (d) indicates the true mode.

TABLE I TRACKING PERFORMANCE IN CASES 1－4

Person #	Case 1	Case 2 [%]	Case 3 [%]	Case 4 [%]
1	0.28	+1.6	-9.0	+77.0
2	0.35	-7.0	-4.7	+37.0
3	0.50	+4.1	+36.3	+48.1
4	0.21	+2.5	+0.4	+22.3
5	0.31	+18.5	-3.8	+3.1
6	0.29	+1.7	-6.1	+110.4
7	0.24	+6.3	-5.3	+16.4
8	0.29	+10.3	-1.9	+55.3
9	0.25	+0.4	+4.7	+521.9
10	0.38	-8.4	-6.3	+38.9
11	0.24	+93.6	-11.7	+31.7
12	0.21	+6.1	-0.7	+45.6
13	0.34	+14.1	-4.1	+14.5
14	0.25	+7.2	-0.2	+11.3
15	0.38	+2.9	0.0	+11.6
16	0.27	-0.2	-2.4	+101.3
17	0.23	+4.1	+0.2	+19.9
18	0.32	-0.6	-12.9	+0.1
19	0.38	-10.7	-7.1	+35.2
20	0.45	+30.8	-8.5	+89.4
Mean	0.31	+8.1	-1.2	+61.2

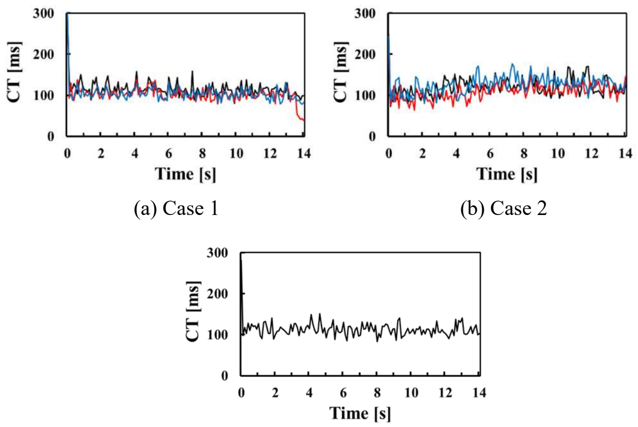

(a) Case 1 (b) Case 2

(c) Case 3

Figure 8. Computation time. The black, red, and blue lines in (a) and (b) indicate the results of LiDARs 1, 2, and 3, respectively.

TABLE II ROOT MEAN SQUARES OF THE COMPUTATION TIME

	LiDAR 1	**LiDAR 2**	**LiDAR 3**
Case 1	114.5 ms	103.9 ms	104.5 ms
Case 2	119.7 ms	109.1 ms	126.5 ms
Case 3	113.4 ms		

The tracking performance in case 4 (DKF-based tracking) is approximately 61% worse than that in case 1 (DIMM-based tracking). This is because, in case 4, a constant-velocity model is employed as the motion model of a person, and the tracking error increases when the person performs a sudden acceleration motion.

We compare the computation time of DIMM-based tracking (cases 1 and 2) and CIMM-based tracking (case 3). The specifications of the computer are Windows 10 Pro OS, Intel(R) Core (TM) i7-8565U@1.80 GHz CPU, 16 GB RAM, and C++ software language. Figure 8 shows the results, and Table II lists the root mean squares of the computation time. The computation time indicates the time required to detect and track people from the LiDAR scan data obtained within a scan. Note that the computation time in case 3 (CIMM-based tracking) is the sum of the computation times in LiDAR 1 and the central server.

The computation time is almost the same for all the cases. Although the computation time should be less than 100 ms of the LiDAR scan period, herein, it is slightly higher than 100 ms. This can be reduced by optimizing the program code and using a graphical processing unit for real-time operations.

VII. CONCLUSION AND FUTURE WORK

This paper presented a cooperative tracking of people using networked LiDARs based on a DIMM estimator. Simulation experiments of tracking of 20 people were conducted using three Velodyne 32-layer LiDARs set in an intersection environment. The tracking performance of the presented method in two different network topologies (ring and line network topologies) was evaluated by comparing the tracking performance of the CIMM and DKF estimators.

DIMM- and CIMM-based tacking showed comparable performance, and the performance of DIMM-based tracking was 61% lower than that of DKF-based tracking. In addition, the computation times for DIMM- and CIMM-based tacking were almost the same.

In our future studies, we will evaluate the presented method through real experiments. In addition, we will employ a machine-learning-based method to improve the performance of people detection in crowded environments.

ACKNOWLEDGMENT

This study was partially supported by the KAKENHI Grant #20H00589, the Japan Society for the Promotion of Science (JSPS).

REFERENCES

[1] A. Brunetti, D. Buongiorno, G. F. Trotta, and V. Bevilacqua, “Computer vision and deep learning techniques for pedestrian detection and tracking: A survey,” Neurocomputing, vol. 300, pp. 17–33, 2018.

[2] E. Marti, J. Perez, M. A. Miguel, and F. Garcia, “A review of sensor technologies for perception in automated driving,” IEEE Intelligent Transportation Systems Magazine, pp. 94–108, 2019.

[3] Md. H. Sharif, “Laser-based algorithms meeting privacy in surveillance: A survey,” IEEE Access, vol. 9, pp. 92394 –92419, 2021.

[4] K. Nakamura, H. Zhao, X. Shao, and R. Shibasaki, “Human sensing in crowd using laser scanners,” Laser Scanner Technology, pp. 15–32, 2012.

[5] T. Wu, J. Hu, L. Ye, and K. Ding, “A pedestrian detection algorithm based on score fusion for multi-LiDAR systems,” Sensors 2021, 21, 1159, 2021.

[6] M. Hashimoto, M. Yuminaka, and K. Takahashi, “Laser-based people tracking system using multiple ground laser scanners,” Proc. of the first IASTED Int. Conf. on Intelligent Systems and Robotics, pp. 95–101, 2016.

[7] E. Mazor, A. Averbuch, Y. Bar-Shalom, and J. Dayan, “Interacting multiple model methods in target tracking: A survey,” IEEE Trans. on Aerospace and Electronic Systems, vol. 34, no. 1, pp. 103–123, 1988.

[8] T. Nakahira, M. Hashimoto, and K. Takahashi, “Cooperative people tracking with multiple ground laser scanners,” Proc. of Int. Symp. on Flexible Automation, 2018.

[9] H. A. P. Blom and Y. Bar-Shalom, “The interacting multiple model algorithm for systems with Markovian switching coefficient,” IEEE Trans. on Automatic Control, vol.33, no.8, pp. 780–783, 1988.

[10] F. F. C. Rego, A. M. Pascoal, P. A. Aguiar, and C. N. Jones, “Distributed state estimation for discrete-time linear time invariant systems: A survey,” Annual Reviews in Control, vol. 48, pp. 36–56, 2019.

[11] C. Y. Chong, K. C. Chang, and S. Mori, “A review of forty years of distributed estimation,” Proc. of 2018 21st Int. Conf. on Information Fusion, 2018.

[12] T. Nakahira, M. Hashimoto, and K. Takahashi, “Cooperative people tracking using multiple ground Lidars based on distributed interacting multimodel estimator,” Proc. of the IEEE 6th 2019 Int. Conf. on Control, Decision, and Information Technologies, 2019.

[13] W. Li and Y. Jia, “Distributed estimation for Markov jump systems via diffusion strategies,” IEEE Trans. on Aerospace and Electronic Systems, vol. 53, pp. 448–460, 2017.

[14] L. Xiao and S. Boyd, “Fast linear iterations for distributed averaging,” Systems & Control Letters, vol. 53, pp. 65–78, 2004.

[15] M. Hashimoto, T. Konda, Z. Bai, and K. Takahashi, “Laser-based tracking of randomly moving people in crowded environments,” Proc. of IEEE Int. Conf. on Automation and Logistics, pp. 31–36, 2010.

[16] H. W. Kuhn, “The Hungarian method for the assignment problem,” Naval Research Logistics Quarterly, vol. 2, no.1–2, pp. 83–98, 1955.

Digital Dataspace and Business Ecosystem Growth for Industrial Roll-to-Roll Label Printing Manufacturing: A Case Study

Parwinder Singh, Nidhi .Nidhi, Justina Karpavice, Michail J. Beliatis, Mirko Presser
Department of Business Development and Technology, Aarhus University, Herning, Denmark
Emails: (parwinder, nidhi, justina, mibel, mirko.presser) - @btech.au.dk,

***Abstract*—Manufacturing industries across the globe are adopting modern technologies rapidly and are now moving towards Industry 5.0. However, many manufacturing units still need to yield their Industry 4.0 level amid reasons including heavy investments in upgrading existing infrastructure and scrapping existing machinery in the name of modern digitalization. These Small and Medium-sized Enterprises (SMEs) need help finding the best-fit technology to meet their business requirement and impact along with the capital to support digitization. In this study, we present one such case of a Danish manufacturing industry, a label printing SME, stranded between conventional technology and a race towards modern digitization. On the one hand, it has old machinery with a large volume of heavy printing and lamination operations with an established customer base. On the other hand, it is willing to digitalize its manufacturing processes (with minimal upgradation in its existing mechanical infrastructure) to enhance its efficiency and sustainability and catch up with the pace of digitalization for further expansion. This can be achieved by nurturing the benefits of digitalization through the latest technologies, such as Enterprise Resource Planning (ERP), Internet of Things (IoT), Edge, Blockchain, Cloud computing, etc. We studied and analyzed the case of the SME in consideration to understand the core requirement and anticipated bottleneck in the process. This paper has presented our findings through related business process flow mappings, challenges, vision, and possible digital architectural solutions using modern-day technologies, scientific approaches and realization tools. These findings and methods will also be value-added and applicable to other SMEs in similar situations. Thus, it enables them to save their Return on Investment (ROI) while adapting to modern technologies with minimal risk, impact and investments.**

***Index Terms*—Architecture, Blockchain, Business Process Mapping, Digitalization, Edge, IoT, Label Printing, Manufacturing, Semantics**

I. INTRODUCTION

The manufacturing industry has been the backbone of any economy across the globe for decades. With the advent of Industry 4.0 [1], the manufacturing industry has focused towards adaptation, automation and data-driven manufacturing operations leveraging modern technologies such as the Internet of Things (IoT) [2], Big Data [3], Enterprise Resource Planning (ERP), Platform Solutions, etc. [4]. The industry is slowly moving towards Industry 5.0, wherein human and machine interaction is a prime focus. However, the Industry 5.0 evolution can only be achieved once Industry 4.0 is adopted, as it addresses the socio-economic impacts of Industry 4.0 on humans [5]. Thus, the manufacturing industry must first achieve the Industry 4.0 goals, which seems way easier for large manufacturing companies because of the available workforce, resources and investments than SMEs. Adopting Industry 4.0 seems strenuous for SMEs as they have limitations with finances, knowledge resources, workforce, and trending technical advances [6].

To deal with similar challenges of SMEs in Denmark, the Danish government has started a growth technology project called Manufactory to boost collaborations between industry and knowledge institutions at a regional level under the supervision of the Danish Industry Foundation [7]. This project has several consortium partners from academia and industry to develop a common platform where both can collaborate and co-create solutions, leveraging modern cutting-edge technologies, to real-world industrial problems (particularly for SMEs). This study results from one such initiative among several taken under this Manufactory project at our Department of Business Development and Technology (BTECH), Aarhus University, - a key academic partner in this project. We collaborated with a Roll-to-Roll (R2R) Label Printing SME with a worldwide clientele base in the Midtjylland area of Denmark. The company got its latest machinery and other infrastructure installed in 2007; thus, the upgradation to modern mechanical infrastructure is not straightforward. However, the SME still has a desire to nurture benefits and cope with modern digitalization to create efficient and value-added expansions, such as data sharing with their customers in real-time, making the production environment smarter and augmenting digitalization slowly and steadily to come up with a differentiator and transformed business model in the Label Printing domain. In this context, for example, IoT technology and related edge network sensing capabilities, such as environmental, print quality, ink toning, bar-code, energy efficiency, predictive maintenance, production line sensing, etc., can streamline operations, improve quality control, enhance supply chain visibility, and reduce costs for the SME. Thus ultimately benefiting both the SME and its customers.

This study summarizes the insights and knowledge acquired while collaborating with the R2R label printing SME through workshops and one-on-one interactions with the company's

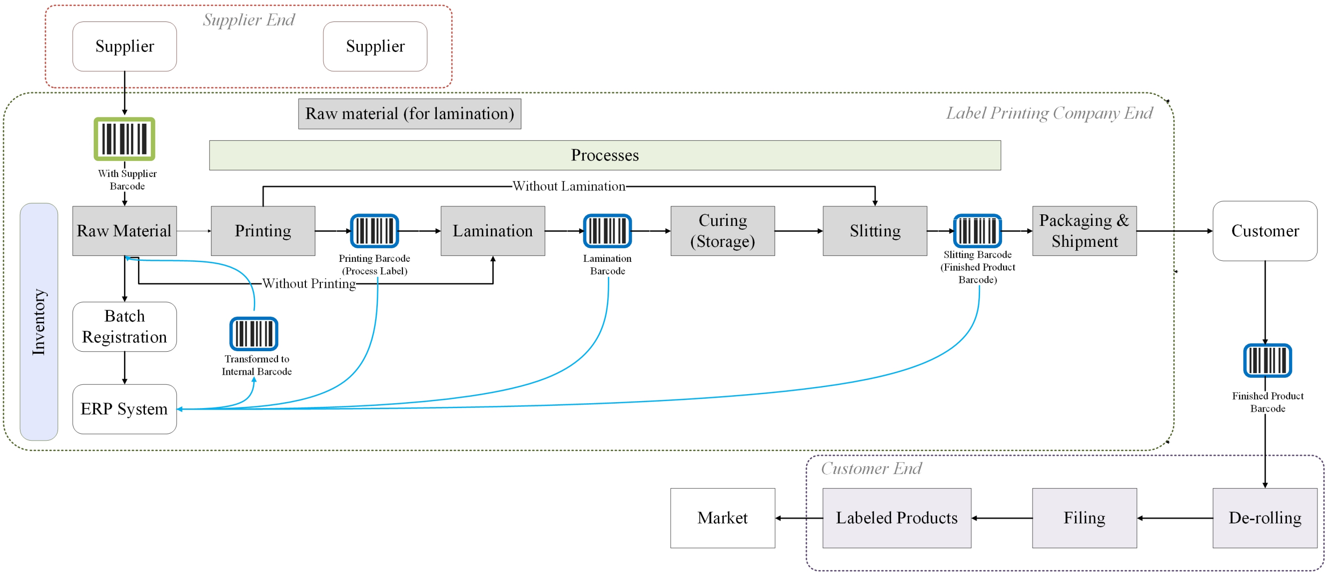

Fig. 1. Business Process Model for the SME workflow

top-level management to understand their business process, perspectives, associated challenges and vision. The study contributes with both business and technical standpoints wherein a business of SME is investigated, which leads to the identification of challenges and process level understanding and results in a system architecture that supports the vision and mission towards digitalization and sustainability.

The rest of the paper is organised as follows: Section II will highlight the background of the label printing industries with associated challenges and our approach to the investigation and analysis. Section III will elaborate on our findings and business propositions, and highlight BPM. Section IV will present the proposed architecture to mitigate and digitize the concern challenge. Finally, Section V will conclude the paper with future opportunities and research scope.

II. Background and Methodologies

The label printing industry is essential in manufacturing for creating labels for varied purposes such as brand promotion, product packaging, information leaflets, etc. These industries are further classified based on the print type, material, and adopted technology. For instance, the labels can be of various types with materials ranging from paper to specialized films, such as pressure-sensitive, shrink sleeves, cut-and-stack, in-mould, etc., employing different print technologies like flexographic, digital, and offset printing [8]. With such exhaustive and complex processes, it is evident that errors in label print manufacturing can disrupt production and affect label quality. Common errors in the print industry include misalignment, colour variations, ink smudging/fading, inconsistent print quality, registration, paper jams, spooling, tearing, adhesive problems, barcode errors, missing labels, material compatibility, poor winding quality, etc. These errors can cascade on SMEs, impacting their operations, customer relationships, costs, and overall business performance [9]. To address these challenges, manufacturers employ quality control, equipment maintenance, and staff training to ensure labels consistently meet quality and accuracy standards. In this realm, the convergence of technologies (e.g., IoT, AI, and Blockchain) and dedicated sensors orchestrates precision and efficiency, from monitoring temperature, humidity and pressure to tracking motion, light and colour functions of label printing. The application of sensors in line with the manufacturing process enables real-time data generation, monitoring and collection to provide efficient label printing and quality control in industrial automation settings.

We adopted Business Process Modeling and Notation (BPMN) models and tools [10] to realize efficiently the SME's process flow. It helped us to identify bottlenecks, challenges, gaps and opportunities to enable digital technologies in SME's environment. In addition, a mix of case study and action research methodologies have been used to conduct our research for this study. We also conducted onsite and offsite workshops with the company's top-level management and researchers from the university as a method of qualitative research to understand, observe, collect, map and analyse the information about the relevant processes, operational flows, challenges and future perspectives. The workshops were conducted openly, focusing on transparent communication, setting clear agenda and objectives, practical use cases and scenarios of the SME, and the participant's presentation, followed by in-person visits to the SME facility, discussions, feedback loop and lots of brainstorming sessions.

III. Business Analysis

The Danish Label Printing SME for our study is a pioneer in flexible packaging employing the Flexo printing technique followed by solvent-free and water-based laminations. The SME also provide customer-ready foils for customers to use on their packaging machines after cutting and adding customized functionalities to the foil, such as micro-perforation, embossing, etc., if requested. Based on the data gathered through the workshops, the process flow was developed to map all the operations and inter-departmental process flows as illustrated in Figure 1. It represents the entities in the supply chain, from raw materials to market-ready finished products, primarily categorized into three clusters: Supplier End, Label Printing Company (i.e., SME) End, and Customer End, as explained below:

- **Supplier End**: Once the raw materials are delivered from the suppliers, the supplier barcode placed on each item is uploaded to the ERP system and then transferred to an internal barcode.
- **Label Printing Company End**: Label manufacturing consists of four main processes: printing, lamination, curing, and slitting. After each process, the new barcode is created, printed and attached to the printed/laminated/slitted reel, except for the curing operation, which needs to be processed separately. Then, the reels, a.k.a bundles, are slitted into smaller reels labelled with the finished product barcode, packaged, and shipped to customers.
- **Customer End**: The received reels of labels are de-rolled and applied to the customer products in distinct techniques concerning the type of the products that must be packaged, i.e., labels can be attached, wrapped, laminated on the product, or filled with the product.

A. Identified Challenges

Flexography, used by the SME, is a well-known printing technique for producing high-quality images and graphics at high printing speed in a versatile and cost-effective way [11]. Although flexography is based on a simple concept of ink transfer, multiple variables affect the final quality of the production, including properties of the plates, anilox rollers, printing pressure, and printing substrates [12]. As a result, the investigated SME faces several challenges related to print defects requiring frequent process stoppages for quality control. The following challenges have been identified as outcomes of our workshops and visits to the SME's facility.

- **Error Management**: The main challenge for the SME, which it wants to address immediately, is error management. During the printing or lamination operation, errors occur and need to be communicated internally and to the customer. For internal communication, two (green and red) labels are used manually to mark the start and end of the material to be scrapped during the slitting processes, shown in Figure 2. Similarly, the external error marking allows SME's customers to manually adjust their filling and packaging operations based on the position of the red label, thus acting as passive markers of errors.
- **Automation of Processes**: The processes at the production line are primarily manual. For instance, the real-time information flow between different production stages and waste management is logged manually. The company's ERP system does not cover all the operational aspects, as upgrading and integrating old machinery infrastructure is challenging, impacting overall productivity efficiency.

Fig. 2. Error in Bundle (Red/Green Label indicators)

- **Reduction in Waste Material**: During printing and lamination operations, the occurred errors result in waste. But no data or logs are maintained for the errors' cause, occurrence or frequency. Therefore, a semantic context awareness-driven digital method enablement must be there to enhance productivity and reduce scraps.
- **Data-driven Compliances and Decision Enablement**: Abiding the Climate Act, Denmark, like other EU countries, aims to significantly reduce greenhouse gas emissions by 50-54% in 2025 and 70% in 2030 compared to 1990 levels [13]. Thus, this necessitates stringent compliance from manufacturing industries, demanding comprehensive data on their operations. The SME is found to be struggling to comply with these requirements due to a lack of data-driven operations.

B. Vision

Our workshops and brainstorming sessions with the SME management highlighted their vision behind the initiative to incorporate and facilitate the convergence of technologies into their existing manufacturing and production lines. The SME expects to digitalize the operations to make their products smarter. For example, the printed bundles have associated a lot of operational data during their printing journey, but it is not captured and thus adds no value. The SME's immediate focus is on error management, a low-hanging fruit where digital operations can be induced as a starting point and scaled incrementally for other challenges. Additionally, they want to develop a data-driven servicing model in future, which can sustain and expand the current business horizon for the SME. Therefore, we proposed a platform model based on which the servitization business model [14] will provide value-chain enablement across customers and also enable them to make their production environment smarter.

 ISBN: 978-1-68558-090-2

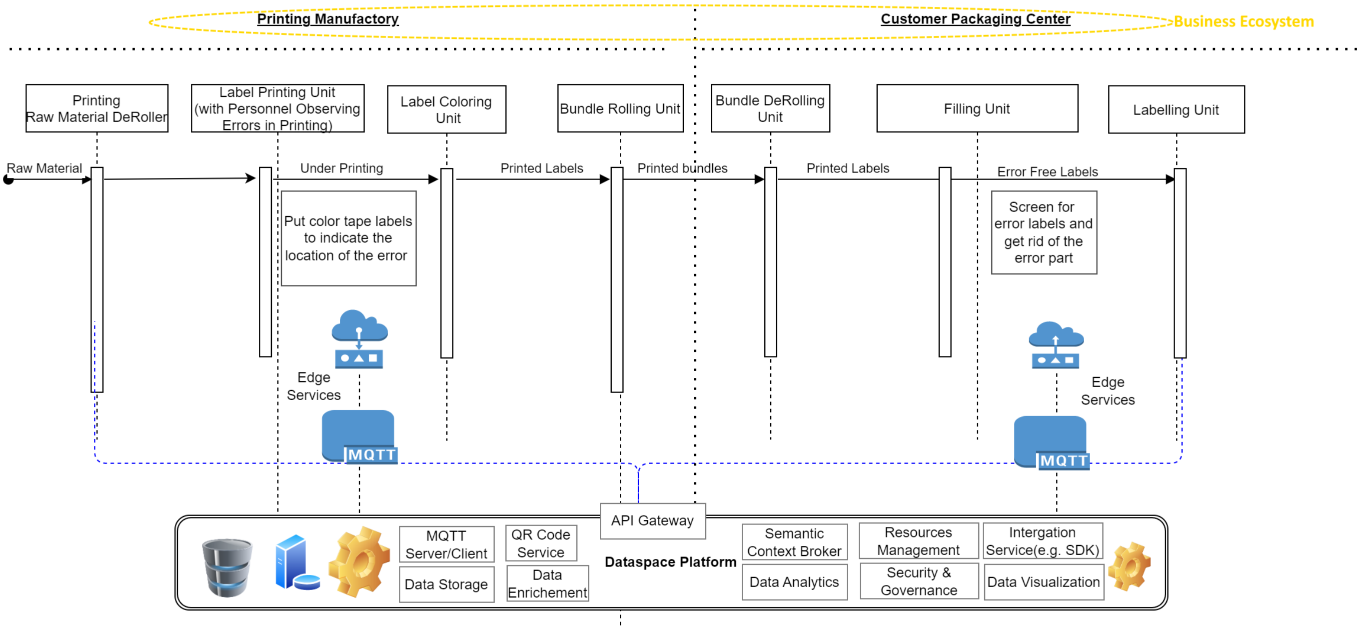

Fig. 3. Digital Intervention Architecture

IV. ARCHITECTURE

This section will primarily provide potential solutions and an architecture to address the identified challenges, focusing on Error Management as the starting point for inducting digital tools in the SME environment. In the present scenario, the entire error identification at its occurrence and relevant communication/action process is handled manually without any digital intervention, giving rise to our problem statement: *"How can we make error management and dependent operations smarter to enhance the overall productivity?"*

Based on our interactions and analysis, we proposed a solution to tackle the challenge of managing errors through the entire workflow and having a log of occurrences. A digital intervention architecture is shown in Figure 3 to address this question. This consists of digital enablement of services at SME and relevant customer on-premises environments, and finally, the Dataspace platform-enabled services provide real-time distributed data services to all the stakeholders. The high-level operational flow of the label printing process is given in the following three steps:

- **Step A**: The Manufacturing Unit receives raw material in huge bundles, each of which goes on the de-rolled roller.
- **Step B**: The de-rolled material goes through the design printing operation, where errors are manually observed during the printing operation and marked with tapes for identification, which is removed later. The error could occur for many reasons, as explained earlier. For instance, when one bundle is finished, it is spliced into a new bundle, and the point of occurrence is notified using tapes. Apart from splicing, errors occur due to printing operations, such as misalignment, colour variations, ink smudging, inconsistent print quality, machine malfunction, etc. To address such errors, we proposed a digital intervention to detect and record the error (explained in the next section).
- **Step C**: At the customer end, the reverse process is repeated to de-roll the bundle and make adjustments on a machine for the error flag in the bundle, and then the error-free labels are split from the bundle and pasted onto the final product.

The above steps have associated data labels as barcodes or manual receipts, but they lack real-time linkage as they flow through the printing operations. Thus, to automate this stage, we propose IoT edge-enabled Quick Response (QR) code-based data labels at all stages of printing operations. We also propose to generate a *"Context-Aware Operational Environment"* and link the information in different functional flows in future during the entire "Order and Error Management" process for the relevant customer. The semantic model can easily capture the business level flow relevant operational context and provides technical implementation grounding at the system level, such as using semantic RDF [15], NGSI-LD [16] or JSON-LD [17] standards. In the following subsections, we have described the applicable process and system model using the semantics ontology approach that can be implemented by the supporting digital platform to induce digitization in the processes.

A. Digital Processing Model for Printings Operations

Figure 4 illustrates the semantic data model for managing printing errors. The *Customer* places an *Order*, which has to be processed with delivery target *Date* by assigning an order identification - *ID*. Similarly, the *ID* property can be used for every operational entity in printing processing. To process this order, there is a need for *Bundle* that contains the raw material for printing with a certain *Length* in meters provided by the customer in his order to print the labels. During the printing operation, there might be *Error* associated, which is identified by an *ID*, defined by its *Metadata*, occurred due to a *Reason* that in turn belongs to a specific *Type* of an *Error*. The printing bundle is finally prepared on specific *Date* for delivery to the customer that receives the final bundle on relevant *Date*.

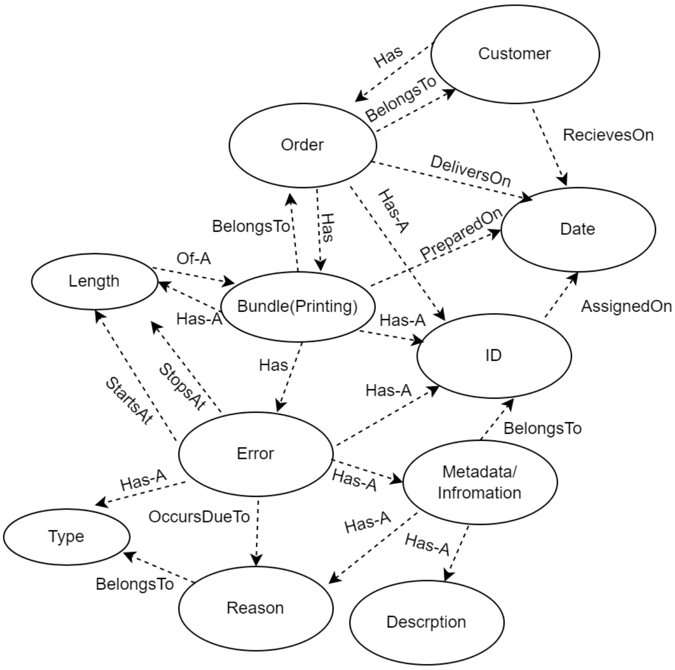

Fig. 4. Semantic Processing Model for Label Printing Operations

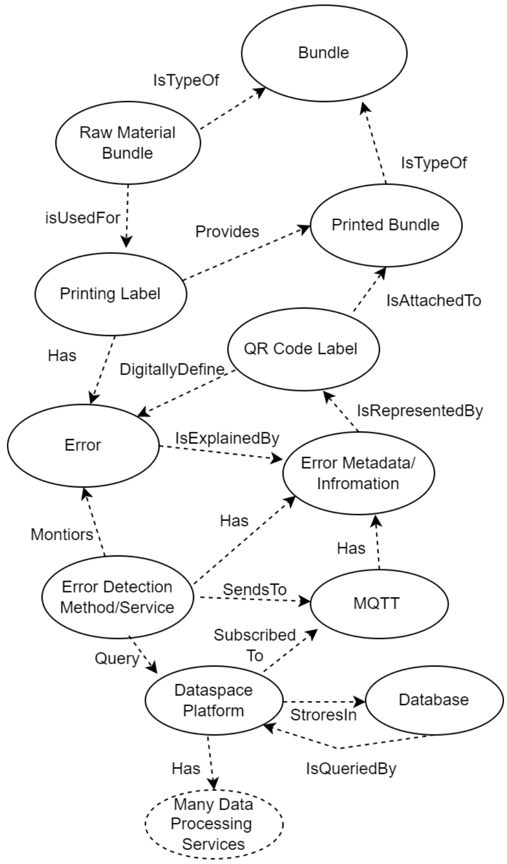

Fig. 5. Semantic System Model

B. Semantic System Model

To initiate digitization, we mapped the SME processes against the digital processes. The system is perceived as a semantic system that provides operational and linked data context awareness [18]. Figure 5 shows the semantic system model that captures the system's relevant operational entity level information. The system focuses on the activities inside a label printing manufacturing unit, that starts with the *Raw Material Bundle*, a type of *Bundle* used for *Printing Label*. During the printing operation, there can be an occurrence of *Error*, which is explained by its metadata that is digitally captured in a *QR Code Label* by the error detection method that also sends the related error information to the *Dataspace* via *MQTT* protocol. In addition, the error method can also query the information from *Dataspace* for various purposes, such as to generate a QR code for encountered errors. At present, the error is monitored manually by personnel of the SME, but in the future, we propose to automate and replace it through edge-enabled (on-premises) IoT sensing and computer vision capabilities. The data received by *Dataspace* platform is persisted in the *Database*, which can be queried later.

C. Dataspace Platform

We propose a platform with Dataspace capabilities [**?**], currently implemented at the university facility, for the SME to prototype and validate its expectations towards initializing digitalization for its error management challenge. The platform is implemented with dataspace capabilities for many reasons: first, the SME management wants to enable digitalization for its processes to augment data-driven decisions over cross-organizational boundaries and thus exploit it as a value addition in their products, i.e., printing bundles, for their business value-chain. For example, the transition of dummy bundles into smart bundles having associated data at the customer end in real-time that can explain the bundle digitally and enable customers to fine-tune their operations and planning accordingly, thus enhancing operational productivity at the customer end. Second, it allows the SME to bring innovation in their business value chain that spans and has an impact at the customer end. This will enable the expansion of SME's portfolio using the platform services model based on smart printing products. Finally, the significant objective for any business is to create monetary opportunities provided by this Dataspace platform, based on the data associated with printing operations. As shown in Figure 3, the Dataspace platform consists of a wide range of data processing services, as explained below.

- **MQTT**: This is an industrial protocol standard [19] that provides standardized push, pull, subscribe or notify data operations. It is widely deployed in the IoT domain that

 ISBN: 978-1-68558-090-2

needs lower resources and power to transmit data over the internet. Though the data model is not standardized at the application level, the communication protocol is standardised. Therefore, context-aware semantic models such as NGSI-LD can be used at the application level.

- **QR Code Service**: This service creates, generates and manages QR codes compatible with various programming languages such as python-qrcode, js-QR in javascript, etc. through open-source libraries. QR codes can be generated from JSON data models, derived from the earlier semantic process model, improving error tagging in manufacturing. This will digitalize the printing operations at each step we explained earlier. In addition, these QR tags can be pushed to the blockchain network to make them digitally traceable and transparent for all stakeholders [20].
- **Data Enrichment**: Inside the platform, this service will allow the modification of received data from the manufacturing unit, e.g., to add a timestamp when the bundle gets its error or when it gets delivered to the customer or error reference modifications or semantic adaptation.
- **Data Storage**: This service allows the data to persist for history and real-time operations among different stakeholders within or across customers of the SME.
- **Semantic Context Broker**: This provides context awareness over the data defined as per the semantic model—for example, the error, length, bundle, customer and delivery relationship. The stakeholder can query the data with a specific context. For example, a customer can ask - *How many and where the errors were when the ordered bundle was printed?*. Under such a scenario, the knowledge base created by a semantic context broker will yield the corresponding query result in a much simplified manner.
- **Data Analytics**: These AI/ML-driven data analytical services can assist SME and customers in their decision-making process. For example, questions like *how many errors have occurred in the last 6 months and how much material has been wasted due to different error types?* can be answered through these services efficiently, and estimated predictive analysis can also be performed.
- **Security and Governance**: This aspect is very important, especially when data and multiple stakeholders are involved. On top of that, GDPR compliances are stringent in Europe for manufacturing units to comply with to avoid hefty fines. This can be implemented using smart contracts among stakeholders, leveraging Blockchain technology such as HyperledgerFabric [21]. This will enable trust through transparency, immutability, digital traceability and tamperproof printing operations. In addition, this service will also provide identity, authentication and authorization management functionality.
- **Resource Management**: This typical ERP-related service manages resources at different operational stages. In addition, this service can also host the responsibility to manage the edge and cloud-level resources consumed by instantiated or orchestrated services. Here, oper-source ERP systems such as Odoo [22] can be very helpful for SMEs to start with.
- **Data Visualization**: This service will provide data visualisation in different formats such as bar charts, line charts, pie charts, heatmaps, 3D charts, Scatter plots, Gantt Charts, etc. Here, open-source tools like Grafana, Elastic Search Logstach Kibana (ELK) stack and industrial tools like Power-BI are heavily used.
- **Integration Service**: This service will provide the required interfaces or Software Development Kit (SDK) to integrate with the Dataspace platform. This will be needed when the SME, under its customer service initiative for its products, say smart bundle, wants to share its operational data with the customer at the customer end so that the customer can align its processing or planning operations accordingly or for other purposes.
- **API Gateway**: This acts as a proxy gateway for the backend microservices running in a distributed environment and thus provides a single point of interaction for the SME or the external world, including customers. This can be implemented using production-grade open-source such as Nginx.

This dataspace platform is recommended to implement following the distributed microservices architectural design approach. This allows the services to be realized at the edge with the IoT sensing capabilities for data generation and processing to optimize bandwidth usage and reduce latency at the edge, i.e., the on-premises environment of the SME. In addition, this can be extended further to integrate the digital twin functionality to achieve operations validation during command and control, higher levels of efficiency, quality, and flexibility. This platform can be deployed on-premises as a private edge cloud and can leverage resources at the cloud level, following the Cloud-Edge continuum hybrid approach [23]. We suggested starting with the edge level deployment to re-use the existing infrastructure to deploy edge cloud leveraging open source Kubernetes-based bare metal microservices oriented containerized approach [24]. Later, as required, it can expand to the public cloud, e.g., AWS, MicrosoftAzure, Google Cloud Platform, etc. This platform enables value-added services across the value chain of the SME by enhancing the label printing process through optimized data-driven real-time operations, ensuring data integrity, and providing powerful analytics and visualization capabilities. This will empower the SME and its customers to make informed decisions, transparency, trust and drive efficiency in label printing operations.

V. CONCLUSIONS AND FUTURE WORK

In this study, we have provided insights on business analysis and digitizing approach for Industrial R2R Label Printing Manufacturing SME in Denmark as part of the Manufactory project. We observed that the SME, operating on a global scale with substantial printing operations and recently installed heavy machinery, faces significant challenges in upgrading its existing infrastructure due to various constraints such as capital investment, resources and affordability. Our approach focused on understanding the intricacies of the SME's operational processes, leading to valuable insights. As a result, we did the business process mapping that provides a better and more precise understanding of enabling data and digitalization points in the existing environment. We identified numerous challenges, including productivity enhancement, error management, communication inefficiencies, waste reduction, compliance requirements, and the potential for smart products through platform-based data augmentation etc. To address these challenges, we narrowed our focus to error management within printing operations and presented a semantic process and system model. We addressed the error management challenge specific to printing operations that can occur for many reasons, e.g., inconsistent material, colour, speed, alignment, etc.) through the induction of digital processes around the same. In addition, we have also proposed a process-mapped architectural solution based on a semantic model that captures the business and technical level aspects concurrently. This proposed solution implementation approach is also explained based on well-defined standards, protocols and an open-source tools ecosystem that requires minimal investments and risks. As an outlook, we would like to measure the impact and value addition of the proposed solution on SME's printing operations to enable digital transformation in business productivity enhancements, reduction in waste material, and expansions through data-driven sustainable growth.

REFERENCES

[1] A. Rojko, "Industry 4.0 concept: Background and overview." *International journal of interactive mobile technologies*, vol. 11, no. 5, 2017.

[2] A. Ghasempour, "Internet of things in smart grid: Architecture, applications, services, key technologies, and challenges," *Inventions*, vol. 4, no. 1, p. 22, 2019.

[3] L. D. Xu and L. Duan, "Big data for cyber physical systems in industry 4.0: a survey," *Enterprise Information Systems*, vol. 13, no. 2, pp. 148–169, 2019.

[4] J. Qin, Y. Liu, and R. Grosvenor, "A categorical framework of manufacturing for industry 4.0 and beyond," *Procedia cirp*, vol. 52, pp. 173–178, 2016.

[5] X. Xu, Y. Lu, B. Vogel-Heuser, and L. Wang, "Industry 4.0 and industry 5.0—inception, conception and perception," *Journal of Manufacturing Systems*, vol. 61, pp. 530–535, 2021.

[6] T. Masood and P. Sonntag, "Industry 4.0: Adoption challenges and benefits for smes," *Computers in Industry*, vol. 121, p. 103261, 2020.

[7] S. Thomsen, *The Danish industrial foundations*. Djøf Forlag, 2017.

[8] B. A. Morris, *The science and technology of flexible packaging: multilayer films from resin and process to end use*. William Andrew, 2022.

[9] C. H. Rao, K. Avinash, B. Varaprasad, and S. Goel, "A review on printed electronics with digital 3d printing: fabrication techniques, materials, challenges and future opportunities," *Journal of Electronic Materials*, vol. 51, no. 6, pp. 2747–2765, 2022.

[10] Y. Odeh, "Bpmn in engineering software requirements: an introductory brief guide," in *Proceedings of the 9th International Conference on Information Management and Engineering*, 2017, pp. 11–16.

[11] Z. Abusaq, S. Zahoor, M. S. Habib, M. Rehman, J. Mahmood, M. Kanan, and R. T. Mushtaq, "Improving energy performance in flexographic printing process through lean and ai techniques: A case study," *Energies*, vol. 16, no. 4, p. 1972, 2023.

[12] D. Valdec, K. Hajdek, L. Vragović, and R. Geček, "Determining the print quality due to deformation of the halftone dots in flexography," *Applied Sciences*, vol. 11, no. 22, p. 10601, 2021.

[13] D. E. Agency, "Denmark's climate status and outlook," Danish Energy Agency, Tech. Rep., 2022.

[14] S. Lamperti, A. Cavallo, and C. Sassanelli, "Digital servitization and business model innovation in smes: A model to escape from market disruption," *IEEE Transactions on Engineering Management*, pp. 1–15, 2023, times cited: 3 event-title: IEEE Transactions on Engineering Management.

[15] R. Angles, H. Thakkar, and D. Tomaszuk, "Rdf and property graphs interoperability: Status and issues." *AMW*, vol. 2369, 2019.

[16] E. CIM, "Ngsi-ld cim 009," ETSI, Tech. Rep., 2019, times cited: 3. [Online]. Available: https://www.etsi.org/deliver/etsigs/CIM.

[17] M. Sporny, D. Longley, G. Kellogg, M. Lanthaler, and N. Lindström, "Json-ld 1.1," *W3C Recommendation, Jul*, 2020.

[18] P. Singh, K. S. Acharya, M. J. Beliatis, and M. Presser, "Semantic search system for real time occupancy," in *2021 IEEE International Conference on Internet of Things and Intelligence Systems (IoTaIS)*. IEEE, 2021, pp. 49–55.

[19] O. Standard, "Mqtt version 5.0," *Retrieved June*, vol. 22, p. 2020, 2019.

[20] P. Singh, K. Holm, M. J. Beliatis, A. Ionita, M. Presser, P. Wolfgang, and R. C. Goduscheit, "Blockchain for economy of scale in wind industry: A demo case," in *Global IoT Summit*. Springer, 2022, pp. 175–186.

[21] A. Srivastava and Y. Desai, "Performance analysis of hyperledger fabric based blockchain for traceability in food supply chain," in *2021 IEEE 2nd International Conference on Technology, Engineering, Management for Societal impact using Marketing, Entrepreneurship and Talent (TEMSMET)*. IEEE, 2021, pp. 1–5.

[22] C. Li, S. Mantravadi, and C. Møller, "Aau open source mes architecture for smart factories–exploiting isa 95," in *2020 IEEE 18th international conference on industrial informatics (INDIN)*, vol. 1. IEEE, 2020, pp. 369–373.

[23] F. Lordan, D. Lezzi, and R. M. Badia, "Colony: Parallel functions as a service on the cloud-edge continuum," in *European Conference on Parallel Processing*. Springer, 2021, pp. 269–284.

[24] A. Orive, A. Agirre, H.-L. Truong, I. Sarachaga, and M. Marcos, "Quality of service aware orchestration for cloud–edge continuum applications," *Sensors*, vol. 22, no. 5, p. 1755, 2022.